

Northumbria Research Link

Citation: Abd El Aziz, Ahmad, Ng, Wai Pang, Ghassemlooy, Zabih, Aly, Moustafa and Chiang, Ming-Feng (2008) Optimisation of the key SOA parameters for amplification and switching. In: Proceedings of the 9th Annual Postgraduate Symposium on the Convergence of Telecommunications , Networking & Broadcasting. PGNET, Liverpool, pp. 107-111. ISBN 978-1902560199

Published by: PGNET

URL:

This version was downloaded from Northumbria Research Link:
<http://nrl.northumbria.ac.uk/id/eprint/2131/>

Northumbria University has developed Northumbria Research Link (NRL) to enable users to access the University's research output. Copyright © and moral rights for items on NRL are retained by the individual author(s) and/or other copyright owners. Single copies of full items can be reproduced, displayed or performed, and given to third parties in any format or medium for personal research or study, educational, or not-for-profit purposes without prior permission or charge, provided the authors, title and full bibliographic details are given, as well as a hyperlink and/or URL to the original metadata page. The content must not be changed in any way. Full items must not be sold commercially in any format or medium without formal permission of the copyright holder. The full policy is available online: <http://nrl.northumbria.ac.uk/policies.html>

This document may differ from the final, published version of the research and has been made available online in accordance with publisher policies. To read and/or cite from the published version of the research, please visit the publisher's website (a subscription may be required.)



**Northumbria
University
NEWCASTLE**



University Library

Optimisation of the Key SOA Parameters for Amplification and Switching

A. Abd El Aziz, W. P. Ng, *Member, IEEE*, Z. Ghassemlooy, *Senior Member, IEEE*, Moustafa H. Aly, *Member, OSA* and M. F. Chiang,

Abstract—This paper presents the effects of the input signal on the gain and carrier density response of a semiconductor optical amplifier (SOA). The SOA is modelled using segmentation method. The optimum bias current required by the SOA for amplification and switching functions are investigated. The operation principle is simulated and the results show the input boundary conditions and requirements in which the SOA can be used as an amplifier and a switch.

Index Terms—semiconductor optical amplifier (SOA), carrier density, stimulated emission, gain response.

I. INTRODUCTION

NOWADAYS, ultrafast photonic networks rely on photonic signal processing to overcome the speed bottleneck imposed by optoelectronic conversions. Optical amplifier is not limited only to amplify optical signals; it is also used as an important element in all-optical switching, regeneration and wavelength conversion. Among all-optical switches, ultrafast all-optical switches based on SOA, such as Mach-Zehnder Interferometers (MZIs) [1] are the most promising candidates for the realization of all-optical switching and processing applications due to their feature small size, high stability, low switching energy, high integration potential and their fast and strong nonlinearity characteristics [2-4]. There are three major nonlinear effects based on SOA; (i) cross-gain modulation (XGM), (ii) cross-phase modulation (XPM) and (iii) four-wave mixing (FWM).

SOA is also a key component for cascaded optical fiber systems and optical gating [5, 6]. Optical gates are needed in most all-optical functions such as wavelength conversion, add-drop multiplexing (wavelength and time), clock recovery, regeneration and simple bit-pattern recognition [7].

Moreover, the use of SOAs as in-line amplifiers is very suitable for bi-directional transmission in local and metropolitan systems and networks because of the lower cost of SOAs and they do not need any optical isolators as often used in different types of amplifiers such as erbium doped fiber amplifiers (EDFAs) [6].

In this paper, optimum parameters required for the SOA are simulated to perform amplification and switching functions. The key optimisations are achieved by controlling the bias current based on the input power to the SOA. The effect of the optimization on the carrier density and the gain responses are investigated. The principle of operation of the SOA is shown in the following section while section III presents the

mathematical analysis of the total gain and the change of the carrier density in terms of the rate equations. In section IV the boundary conditions and requirements for the SOA to perform amplification and switching are presented. The final section concludes the findings of the investigation.

II. SOA PRINCIPLE OF OPERATION

The basic structure of the SOA is a semiconductor laser composed of an optical waveguide between a P-N junction with an input and output coated facets as displayed in Fig. 1 [8]. When a direct current (DC) is biased to the SOA, electrons get higher energy. Hence, the conduction and valence bands (energy levels) containing electrons and holes, respectively are formed [9].

The formation of these energy levels results in three radiative mechanisms within the SOA:

i. Spontaneous emission; which is the process where an electron from the conduction band drops to the valence band releasing a photon or generating heat. This process is considered as loss or noise because the generated photon is radiated with different phase and direction.

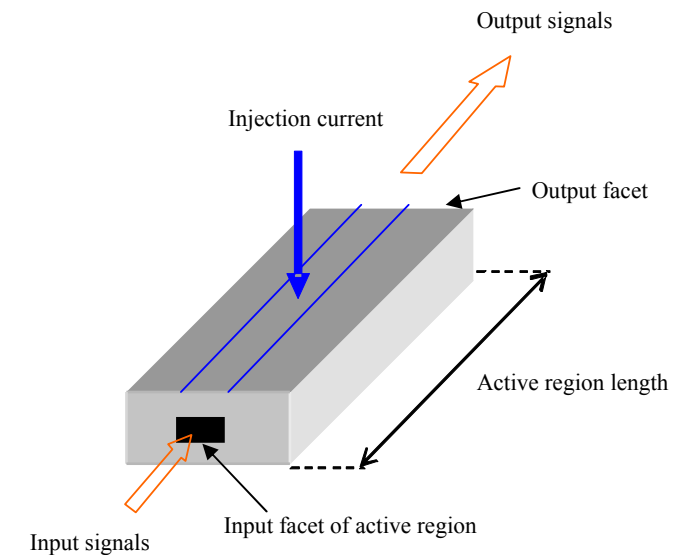


Fig. 1. Schematic diagram of the SOA.

ii. Stimulated absorption; this is the process by which an electron in the valence band absorbs enough energy from an incident photon to pass the energy gap to the conduction band and hence causes loss.

iii. Stimulated emission; this process occurs when an incoming optical beam is launched into the active waveguide of the SOA via the input facet of the amplifier, an incident photon collides with an excited electron from the conduction band releasing a stimulated photon with the same phase, frequency and direction (i.e. amplification takes place). More identical photons are released by the collision of the incident beam of photons with more excited electrons in the conduction band thus amplifying the input signal [9].

The reduction of excited electrons in the conduction band (i.e. the carrier density) will result in a decrease in the SOA gain because the gain is proportional to the carrier population. Moreover, it will increase the active refractive index due to the nonlinear refractive index being dependent on the carrier density [10, 11].

When a short input optical pulse is launched into the SOA, stimulation emission will take place resulting in signal amplification. Therefore, the carrier density will be reduced and will cause a drop in the SOA gain. The carrier non-equilibrium is governed mainly by the spectral hole burning effect [12, 13]. The distribution recovers to equilibrium by carrier-carrier scattering. Instantaneous mechanisms such as two-photon absorption [14, 15] and the optical Kerr effects [16, 17] will then influence on the SOA response. After few picoseconds, a quasi-equilibrium distribution will occur due to the carrier temperature relaxation process and then the carrier density will be recovered [9].

III. MATHEMATICAL MODEL

The rate equations in small segments in an SOA are iteratively calculated while taking the carrier density change and the SOA length in account [18].

Rate Equations

When light is injected into the SOA, changes occur in the carrier and photon densities within the active region of the SOA. These changes can be described using the rate equations. The gain medium of the amplifier is described by the material gain coefficient, g (per unit length) which is dependent on the carrier density N and is given by [9]:

$$g = \alpha_g (N - N_0), \quad (1)$$

where N_0 is the carrier density at transparency point and α_g is the differential gain parameter. The net gain coefficient g_T is defined by:

$$g_T = \Gamma \cdot g - \alpha_s, \quad (2)$$

where α_s is the internal waveguide scattering loss, and Γ is the confinement factor which is the ratio between the cross-

sectional area of the active medium and the transverse area of the optical waveguide.

The total gain G of an optical wave experienced at the location z of an SOA can be calculated according to

$$G = e^{g_T z}, \quad (3)$$

assuming a constant carrier density at any given location z within the active region of the SOA.

Therefore, the average output power P_{av} over the length of the SOA becomes:

$$P_{av} = \frac{1}{L} \int_0^L P_{in} G dz, \quad (4)$$

where L is the length of the SOA and P_{in} is the input signal power. The average output power can be rewritten as [19]:

$$P_{av} = P_{in} \frac{e^{g_T L} - 1}{g_T \cdot L}. \quad (5)$$

The dynamic equation for the change in the carrier density within the active region of the device is given by:

$$\frac{dN}{dt} = \frac{I_{DC}}{q \cdot V} - R(N) - \frac{\Gamma \cdot g \cdot P_{av} \cdot L}{V \cdot h \cdot f}, \quad (6)$$

where I_{DC} is the DC current injected to the SOA, q is the electron charge and V is the active volume of the SOA,

$$V = L \cdot W \cdot H, \quad (7)$$

where W and H denote the width and the thickness of the active region, respectively. $R(N)$ is the recombination rate, h is the Planck constant and f is the light frequency.

There are two mathematical definitions for the recombination rate. The simple definition is given by:

$$R(N) = \frac{N}{T_{sp}}, \quad (8)$$

where T_{sp} is the spontaneous emission time and is given by:

$$T_{sp} = \frac{q \cdot V \cdot N_0}{I_{DC}}, \quad (9)$$

while the more complex form is called the Auger recombination and is given by:

$$R(N) = A \cdot N + B \cdot N^2 + C \cdot N^3, \quad (10)$$

where A is the surface and defect recombination coefficient, B is the radiative recombination coefficient and C is the Auger recombination coefficient. In this paper, the Auger recombination equation shown in (10) is used in developing the theoretical SOA model.

IV. RESULTS AND DISCUSSION

The rate equations shown in section III are carried out via MatlabTM to investigate the gain response of the SOA model while employing the segmentation method. The standard SOA parameters used are given in Table I.

The segmentation method involves dividing the SOA into five equally segments of length $l=L/5$ each. The carrier density is assumed to be constant within a segment. However, the carrier density changes from one segment to another depending on its input power and the carrier density of the previous segment using equation (6). In all the equations in section III, the segment length l will replace the SOA length L for the segment total gain and carrier density calculations.

Figure 2 shows the normalized gain response of the SOA using the physical parameters in Table I. As it can be seen, the gain of the SOA increases rapidly until a steady state value where it becomes constant. This increase is due to the injection of the bias current to the SOA hence resulting in a large number of electrons to overcome the energy gap to reach the conduction band. Therefore, the carrier density of the SOA will increase and hence the total gain of the SOA.

TABLE I
Physical parameters of the SOA

parameter	symbol	value/unit
Carrier density at transparency	N_0	$1.4 \times 10^{24}/\text{m}^3$
Initial carrier density	N_i	$3 \times 10^{24}/\text{m}^3$
Differential gain	α_g	$2.78 \times 10^{-20} \text{ m}^2$
Internal waveguide scattering loss	α_s	$40 \times 10^2/\text{m}$
SOA length	L	$500 \mu\text{m}$
SOA width	W	$3 \mu\text{m}$
SOA height	H	80 nm
Confinement factor [20]	Γ	0.3
Light frequency	f	193.1 THz
Plank constant	h	$6.62606896 \times 10^{-34}$
Electron charge	q	$1.602 \times 10^{-19} \text{ C}$
Surface and defect recombination coefficient	A	$1.43 \times 10^8 \text{ 1/s}$
radiative recombination coefficient	B	$1 \times 10^{-16} \text{ m}^3/\text{s}$
Auger recombination coefficient	C	$3 \times 10^{-41} \text{ m}^6/\text{s}$

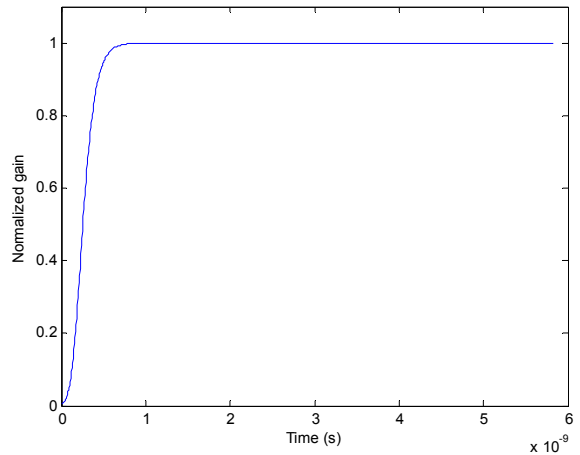


Fig. 2. Normalized gain response of the SOA.

In this simulation, two types of input signals are applied to the SOA separately for investigation. The first input is a short pulse input signal with a pulse width of l/v_g (i.e. 1.1667 ps), where v_g is the group velocity. As explained previously in section II, when the input pulse is injected to the active region of the waveguide, the total gain of the SOA will drop instantly and then will recover back to its steady state value as shown in Fig. 3. The drop of the total gain depends on the power and pulse width of the input pulse as will be discussed at the end of this section.

The second input signal is a continuous wave (CW) signal which will be launched into the SOA after the total gain reaches its steady state value. When a CW is injected into the SOA, the SOA gain will reduce until it reaches a saturation value where the gain becomes constant as shown in Fig. 4. The reason for such response is that a depletion of the carrier density happens due to the continuous stimulation emission process. The carrier density continues to decrease and hence the gain until excited electrons in the conduction band are no longer available. By using the segmentation method, the change of the carrier density along the SOA length after applying the CW can be investigated, as depicted in Fig. 5. Carriers are depleted and therefore gain is suppressed.

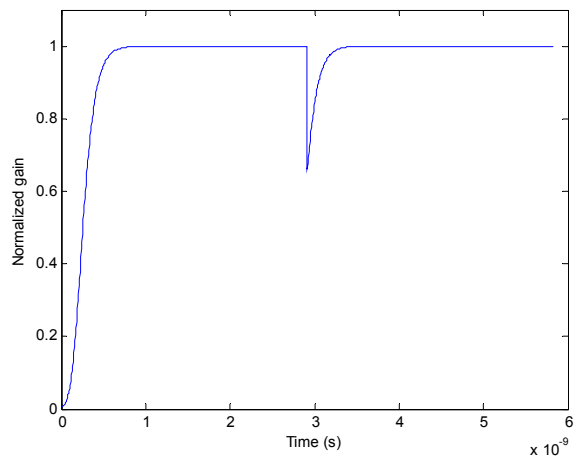


Fig. 3. Normalized gain response of the SOA due to the injection of a short input pulse.

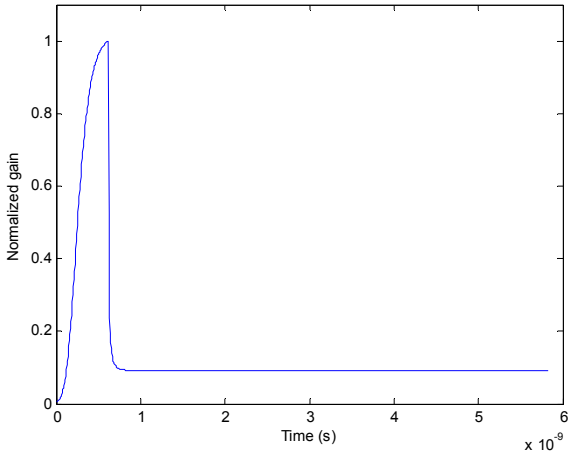


Fig. 4. Normalized gain response of the SOA due to the injection of a continuous input signal.

In order to use the SOA as an amplifier, we should ensure that the signal will not be affected by the SOA nonlinear response which occur when the gain is saturated. This amplification can only be achieved if the SOA gain does not reach its saturation value that is shown in Fig. 4 when applying an input signal pulse. In this paper, the saturation value for a 1mW continuous input signal is used as the reference saturation gain value in which the SOA will achieve a linear response for amplification function.

From Fig. 6 for a given input signal power, one can choose the optimum bias current in order to achieve the required output gain. As expected, the increase of the input signal power results in the decrease of the output gain to a constant minimum gain. For the different values of the bias current, the minimum gain is different. Input signal of 1mW with $I = 250\text{mA}$ achieves a high gain compared to signals with higher input signal power and to signals with lower bias current. This is because higher bias current gives more electrons enough energy to reach the conduction band and hence higher carrier density and higher output gain.

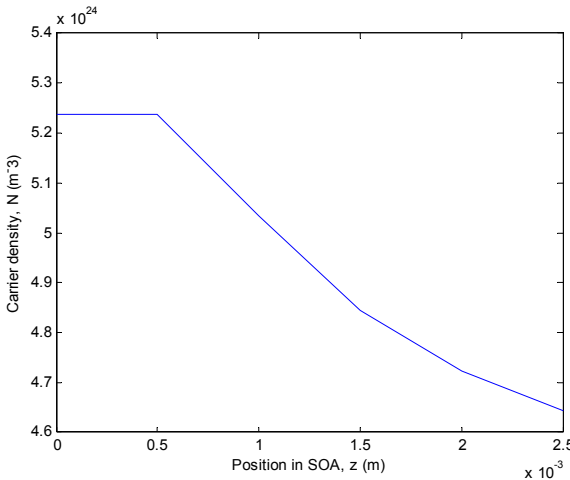


Fig. 5. Carrier density along the SOA length after applying a CW.

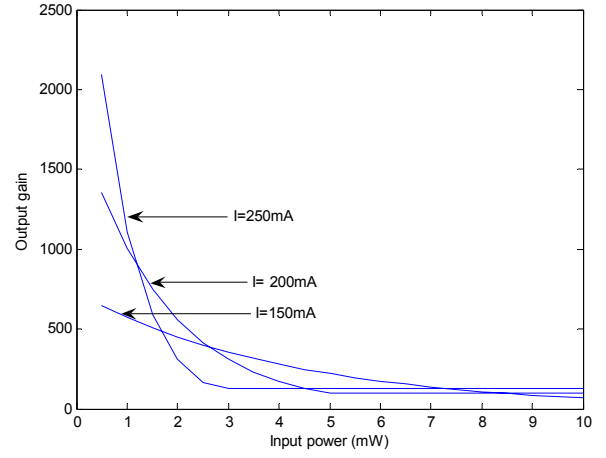


Fig. 6. The output gain corresponding to the input power at different bias currents.

Figure 6 also shows that the rate of decrease of the output gain is the highest in the case of $I = 250\text{mA}$ while it is the lowest in the case of $I = 150\text{mA}$. The reference saturation gain of the SOA at 1mW continuous input signal is 66, 96 and 127 for bias currents of 150mA, 200mA and 250mA, respectively.

On contradictory, in order to use the XPM introduced by SOA for switching function [21], ideally the signal should be affected by the nonlinearity of the SOA and achieve a 180° phase shift for the deconstructive interference [21]. This can be obtained by the aid of a control pulse (CP) which is injected to the active region of the SOA in order to achieve a gain depletion that reaches the gain saturation value. When the total gain reduction reaches this value, a phase shift of 180° will occur [22] and then the input signal should be launched into the SOA in order to achieve this phase shift.

For any input signal to achieve the nonlinear response of the SOA, a corresponding CP is required to drive the total gain of the SOA into the SOA gain saturation. Figure 7 illustrates the corresponding CP power needed by a range of input signal powers to obtain the desired phase shift for different injection currents.

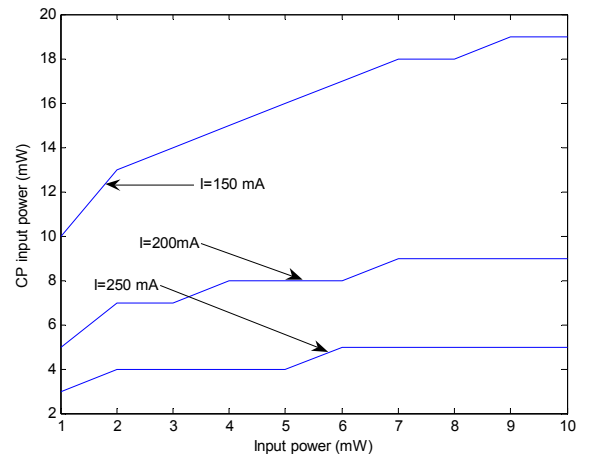


Fig. 7. The saturation CP for corresponding input power at different bias currents.

In Fig. 7, some input signal power would require the same CP power to drive the SOA into saturation, i.e. input power of 6 to 10 mW required CP of 5 mW at $I = 250$ mA. In addition, the CP power required is higher for $I = 150$ mA compared to higher bias currents while for $I = 250$ mA a lower control pulse power is required to drive the SOA into saturation and hence perform switching function [22]. The highest control pulse power needed is of 19mW for an input signal power of 10mW at a bias current of 150mA. On the other hand, the lowest control pulse power needed is 3mW for an input of 3mW at a bias current of 250mA.

V. CONCLUSION

This paper has simulated the total gain response of an SOA model using segmentation method. Continuous and short input signals were applied to the segmentized SOA model to investigate the corresponding gain response in order to achieve amplification and all-optical switching operation respectively. The optimum performance conditions are investigated in this paper for the SOA to function as an amplifier and a switch.

REFERENCES

- [1] S. Nakamura, K. Tajima, and Y. Sugimoto, "Experimental investigation on high-speed switching characteristics of a novel symmetric Mach-Zehnder all-optical switch," *Applied Physics Letter*, vol. 65, pp. 283-385, 1994.
- [2] R. Giller, R. Manning, and D. Cotter, "Gain and phase recovery of optically excited semiconductor optical amplifiers," *IEEE photonics technology letters*, vol. 18, pp. 1061-1063, 2006.
- [3] J. Moerk, M. Nielsen, and T. Berg, "The dynamics of semiconductor optical amplifiers-modeling and applications," *Optics and Photonics News*, vol. 14, pp. 42-48, 2003.
- [4] E. Tangdiongga, Y. Liu, H. Waardt, G. Khoe, A. Koonen, and H. Dorren, "All-optical demultiplexing of 640 to 40 Gbits/s using filtered chirp of a semiconductor optical amplifier," *Optics Letters*, vol. 32, pp. 835-837, 2007.
- [5] J. Yu, A. Buxens, A. Clausen, and P. Jeppesen, "16 x 10 Gb/s WDM bidirectional gating in a semiconductor optical amplifier for optical cross connects exploiting network connection symmetry," *IEEE Photonics Technology Letters*, vol. 12, pp. 702-704, 2000.
- [6] J. Yu, Y. Yeo, O. Akanbi, and G. Chang, "Bi-directional transmission of 8 X 10Gb/s DPSK signals over 80 km of SMF-28 fiber using in-line semiconductor optical amplifier," *Optics Express*, vol. 12, pp. 6215-6218, 2005.
- [7] K. Stubkjaer, "Semiconductor optical amplifier-based all-optical gates for high-speed optical processing," *IEEE Journal on Selected Topics in Quantum Electronics*, vol. 6, pp. 1428-1435, 2000.
- [8] G. Keiser, *Optical fiber communication*. Singapore: McGraw-Hill, 2000.
- [9] H. Le Minh, "All-optical router with PPM header processing high speed photonic packet switching networks," Northumbria University, 2007.
- [10] G. Agrawal and N. Olsson, "Self-phase modulation and spectral broadening of optical pulses in semiconductor laser amplifiers," *IEEE journal on selected topics in quantum electronics*, vol. 25, pp. 2297-2306, 1989.
- [11] M. Eiselt, W. Pieper, and H. Weber, "SLALOM: Semiconductor laser amplifier in a loop mirror," *IEEE journal of lightwave technology*, vol. 13, pp. 2099-2112, 1995.
- [12] L. Guo and M. Connelly, "All-optical AND gate with improved extinction ratio using signal induced nonlinearities in a bulk semiconductor optical amplifier," *optics Express*, vol. 14, pp. 2938-2943, 2006.
- [13] P. Borri, W. Langein, J. Hvam, F. Heinrichsdorff, M. Mao, and D. Bimberg, "Spectral hole-burning and carrier-heating dynamics in quantum-dot amplifiers: comparison with bulk amplifiers," *physica status solidi*, vol. 224, pp. 419-423, 2001.
- [14] H. Ju, A. Uskov, R. Notzel, Z. Li, J. Vazquez, D. Lenstra, G. Khoe, and H. Dorren, "Effects of two-photon absorption on carrier dynamics in Quantum-dot optical amplifiers," *applied physics B. lasers and optics*, vol. 82, pp. 615-620, 2006.
- [15] K. Tajima, S. Nakamura, and Y. Ueno, "semiconductor nonlinearities for ultrafast all-optical gating," *measurement science and technology*, vol. 13, pp. 1692-1697, 2002.
- [16] G. Agrawal, *Nonlinear fiber optics*, 2 ed. San Diego, USA: Academic Press, 1995.
- [17] J. Mendoza-Alvarez, L. Coldren, A. Alping, R. Yan, T. Hausken, K. Lee, and K. Pedrotti, "Analysis of depletion edge translation lightwave modulators," *IEEE journal of lightwave technology*, vol. 6, pp. 793-807, 1988.
- [18] M. Hattori, K. Nishimura, R. Inohara, and M. Usami, "Bidirectional data injection operation of hybrid integrated SOA-MZI all-optical wavelength converter," *Journal of Lightwave Technology*, vol. 25, pp. 512-519, 2007.
- [19] VPIsystems, *VPI transmission maker and VPI component maker: photonic modules reference manual*, 2001.
- [20] F. Tabatabai and H. S. Al-Raweshidy, "Feedforward linearization technique for reducing nonlinearity in semiconductor optical amplifier," *Journal of Lightwave Technology*, vol. 25, pp. 2667-2674, 2007.
- [21] M. F. Chiang, Z. Ghassemlooy, W. P. Ng, and H. Le Minh, "Simulation of an all-optical 1 x 2 SMZ switch with a high contrast ratio," *Proceeding of the 8th annual PostGraduate Symposium on the convergence of Telecommunications, Networking and Broadcasting (PGNET 2007)*, pp. 65-69, 2007.
- [22] Z. Ghassemlooy, W. P. Ng, and H. Le Minh, "BER performance analysis of 100 and 200 Gb/s all-optical OTDM node using symmetric Mach-Zehnder switches," *IEE proceedings Circuit, Devices and Systems on Commun. Systs. Network and DSP*, vol. 153, pp. 361-369, 2006.